Title

Charge ordering and magnetoresistance in Nd1-xCaxMnO3 due to reduced double exchange

Journal

Physical Review B, 54(5)

ISSN

2469-9950

Authors

Liu, K
Wu, XW
Ahn, KH
et al.

Publication Date

1996-08-01

DOI

10.1103/physrevb.54.3007

Peer reviewed

Charge ordering and magnetoresistance in $Nd_{1-x}Ca_xMnO_3$ due to reduced double exchange

K. Liu, X. W. Wu, K. H. Ahn, T. Sulchek, and C. L. Chien
Department of Physics and Astronomy, The Johns Hopkins University, Baltimore, Maryland 21218

John Q. Xiao
Department of Physics and Astronomy, University of Delaware, Newark, Delaware 19716
(Received 9 February 1996; revised manuscript received 11 April 1996)

Structural, transport, and magnetic properties of $Nd_{1-x}Ca_xMnO_3$ ($0 \leqslant x \leqslant 1$) have been studied to probe the consequence of strong lattice distortion and reduced double exchange. Charge ordering has been observed over a large composition range of $0.30 \leqslant x \leqslant 0.80$. For $0.33 \leqslant x \leqslant 0.40$, at low temperatures, a magnetic field induces a first-order antiferromagnetic semiconductor to ferromagnetic metal transition and reduces the resistance by several orders of magnitude. These results illustrate the competition between double exchange and mechanisms that promote charge localization. [S0163-1829(96)07630-8]

Recently, there has been intense interest[1] in the properties of doped $LaMnO_3$ (ABO_3-type) perovskites, prompted by the observation of colossal magnetoresistance (CMR) and other intricate physical properties. In the Mn^{3+} ions, the three t_{2g} electrons form an inert spin core, while the e_g electron is electronically active with its spin parallel to the core spin. Upon doping La at the A sites by divalent ions (e.g., Ba, Sr, and Ca), both Mn^{3+} and Mn^{4+} are present. The e_g electron can now hop between neighboring Mn^{3+} and Mn^{4+} ions via the double-exchange (DE) mechanism.[2] This hopping process critically depends on the relative alignment of the Mn core spins. Consequently, the electrical resistivity is extremely sensitive to the external magnetic field, thus giving rise to CMR.

The geometry of the Mn-O-Mn bond plays a crucial role since the oxygen ion mediates the DE. In an ideal perovskite structure, the Mn ions occupy the centers of the oxygen octahedrons with a 180° Mn-O-Mn bond angle. Distortion of the crystal structure results in buckling of the octahedral network,[3] thereby altering the Mn-O-Mn bond angle and bond distance, affecting the electron hopping probability and the DE interaction. Hwang *et al.*[4] recently demonstrated these lattice effects (e.g., increase in resistivity and CMR, lowering of Curie temperature) through increased lattice distortion.

Millis *et al.*[5,6] have shown that certain key aspects of CMR cannot be accounted for by DE alone. They suggest that a strong electron-phonon coupling, neglected in the original DE theory,[2] should be included. The essential consequence is the formation of Jahn-Teller polarons, a process that tends to localize the e_g electrons. Experimentally, evidence of real space charge ordering,[7–10] large magnetoelastic effects, and field-induced structural phase transitions[11,12] have been reported. These studies, mainly in La-based manganites, suggest charge-lattice (e.g., electron-phonon) and spin-lattice (e.g., magnetoelastic effect) coupling as integral parts of the essential mechanism responsible for the fascinating physics. To study the relative importance of DE and other mechanisms, we have selected the $Nd_{1-x}Ca_xMnO_3$ system. The replacement of La by the smaller Nd introduces a larger lattice distortion, thus weakening the DE. Therefore the effects of electron-phonon coupling, Coulomb interaction, and antiferromagnetic (AF) superexchange can be highlighted.

A series of samples of $Nd_{1-x}Ca_xMnO_3$ ($0 \leqslant x \leqslant 1$) were prepared through the conventional solid-state reaction method. Detailed sample fabrication conditions will be published elsewhere.[13] Because the valence of Mn is of crucial importance, we have used a ferrous sulfate and potassium permanganate titration method to independently determine the content of Mn^{3+}/Mn. The results, shown in Fig. 1(a), exhibit very good agreement with the ideal stoichiometry (dashed line).

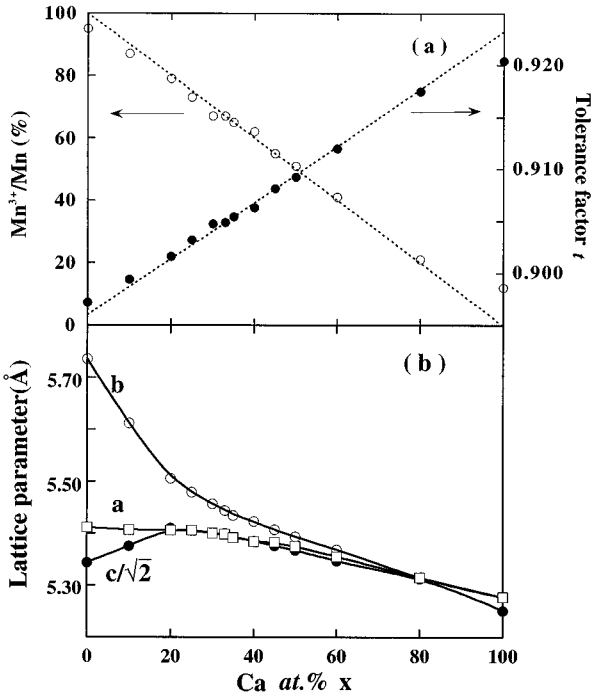

FIG. 1. Variations of (a) Mn^{3+} concentration (open circles) and tolerance factor t (solid circles) and (b) lattice parameters with Ca at. % x in $Nd_{1-x}Ca_xMnO_3$. Dashed lines correspond to ideal stoichiometry.

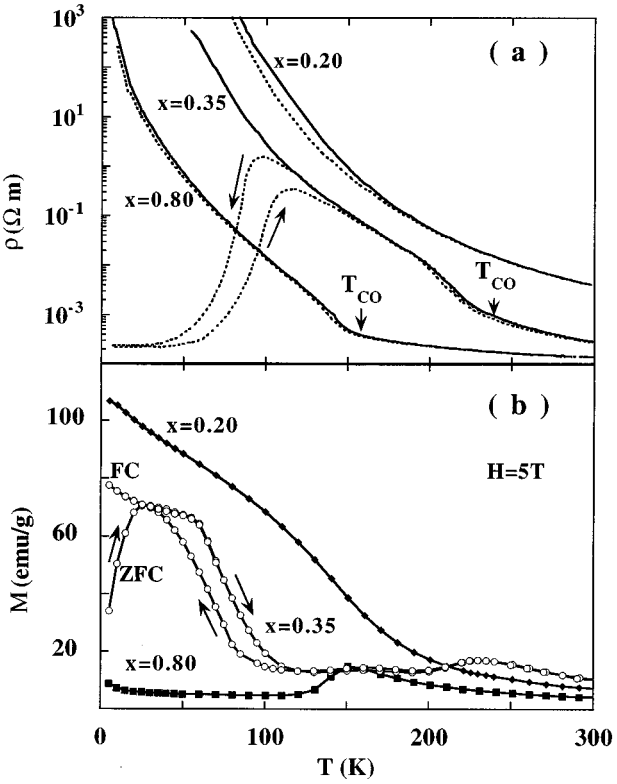

FIG. 2. Representative results of temperature dependence of (a) resistivity ρ in zero field (solid line) and 5 T (dashed line) and (b) magnetization M in a 5 T field for $x=0.20$, 0.35, and 0.80.

X-ray diffraction shows that the samples are of single phase. As Ca doping increases, the crystal structure systematically changes from orthorhombic ($0\leqslant x\leqslant 0.60$) to tetragonal ($0.60<x\leqslant 1$), as shown in Fig. 1(b). To characterize the deviation from ideal perovskite structure, we have calculated the tolerance factor $t=(r_{\mathrm{Nd/Ca}}+r_{\mathrm{O}})/\sqrt{2}(r_{\mathrm{Mn}}+r_{\mathrm{O}})$ for all samples based on the stoichiometry and tabulated radii.[14] The values of t are indeed smaller than those in La/Pr-based systems,[4] indicating a larger lattice distortion. Overall, t increases linearly with Ca concentration as shown in Fig. 1(a).

The temperature dependence of resistivity (ρ) and magnetization (M) for representative samples with $x=0.20$, 0.35, and 0.80 is shown in Fig. 2. A strong correlation between the temperature dependence of the resistivity and magnetization is evident. In Fig. 2(a), the results for $H=0$ and $H=5$ T are shown as solid and dashed lines, respectively. For samples with $0\leqslant x\leqslant 0.25$, semiconducting behavior with activation characteristics is observed. At low temperature, the application of a 5 T field causes significant reduction in ρ, hence a sizable magnetoresistance effect, while the sample remains semiconducting. Magnetically, these samples exhibit a paramagnetic (PM) to ferromagnetic (FM) transition. For samples with $x>0.80$, a PM to AF transition is observed, while the samples also remain semiconducting. No appreciable magnetoresistance is seen.

The samples with $0.30\leqslant x\leqslant 0.80$ show a rich variety of phenomena. They are again semiconductors in zero magnetic field. There is a sudden increase in ρ below a temperature of T_{CO}, at which the magnetization correspondingly shows a peak (T_{CO} will later be identified as the charge ordering temperature). Magnetically, they undergo a PM to AF transition at a temperature $T_N<T_{\mathrm{CO}}$ in zero field. Interestingly, the application of a magnetic field *induces* a simultaneous semiconductor-metal and AF-FM transition only for samples with $0.33\leqslant x\leqslant 0.40$ at low temperatures. CMR of large magnitude is seen in the composition range of $0.30\leqslant x\leqslant 0.45$, while no appreciable MR is present in the range of $0.45<x\leqslant 0.80$.

In the following, we concentrate only on the sample with $x=0.35$. As shown in Figs. 2(a) and 2(b), the sample has $T_{\mathrm{CO}}\approx 240$ K in zero field. At low temperatures, AF behavior and spin canting have been observed. The zero-field resistivity $\rho(0)$ increases monotonically with decreasing temperature and reaches about 10^3 Ω m at 50 K, below which $\rho(0)$ is so large that it has exceeded our measuring limit. Under an external field of 5 T, the resistivity decreases by more than *seven* orders of magnitude to $\rho(5\ \mathrm{T})\approx 10^{-4}$ Ω m at low temperature, exhibiting one of the largest magnitudes of CMR. The sharp drop in ρ, i.e., CMR, is accompanied by a field-induced magnetic transition from AF to FM, as indicated by the zero-field-cooled (ZFC) and field-cooled (FC) magnetization curves in Fig. 2(b). This magnetic transition is first order in nature, signified by pronounced temperature hysteretic effects.

The striking difference between results of Nd-based and those of La-based materials in the similar doping range should be noted. In $\mathrm{La}_{1-x}\mathrm{Ca}_x\mathrm{MnO}_3$ ($0.20\leqslant x\leqslant 0.45$),[15] metallic conduction and ferromagnetism (mediated by DE) occur *spontaneously* below the Curie temperature T_c. CMR arises from the abrupt increase in electron hopping via DE at the onset of the spontaneous FM ordering. Sizable CMR exists in a narrow temperature range near T_c. In Nd-based materials, neither metallic conduction nor ferromagnetism is observed in zero field. CMR originates from the *field-induced* simultaneous semiconductor-metal and AF-FM transitions, and exists over an extended temperature range. The present Nd series also shows higher resistivity, larger magnetoresistance, and stronger temperature hysteresis.

Direct evidence of charge ordering (CO) has been observed by electron diffraction in the $x=0.35$ sample. Diffraction patterns have been obtained from a single grain along the [001], [100], and $[\bar{1}10]$ zone axes. At room temperature, diffraction patterns show that the structure is essentially tetragonal ($a\approx b=5.4$ Å, $c=7.6$ Å), consistent with the small orthorhombic distortion seen by x-ray diffraction. The same patterns have been observed at 250 K, as shown in Figs. 3(a) and 3(b) along the [001] and [100] zone axes, respectively. At 170 K, however, strikingly different features of additional superlattice spots appear, as shown in Figs. 3(b) and 3(d). Moreover, in the pattern taken along the [001] zone axis [Fig. 3(b)], the superlattice spots appear along both the [100] and [010] directions, whereas in the pattern taken along the [100] zone axis [Fig. 3(d)], the spots appear only in the [010] direction. These results demonstrate charge ordering with uniquely defined modulation wave vectors of $\mathbf{q}=(2\pi/a)(\frac{1}{2},0,0)$ and $\mathbf{q}=(2\pi/a)(0,\frac{1}{2},0)$. Both of these wave vectors allow diffraction along the [001] zone axis, and only the latter facilitates diffraction along the [100] zone axis. The absence of superlattice spots in the third zone axis of $[\bar{1}10]$ further confirms the conclusion. These results show that

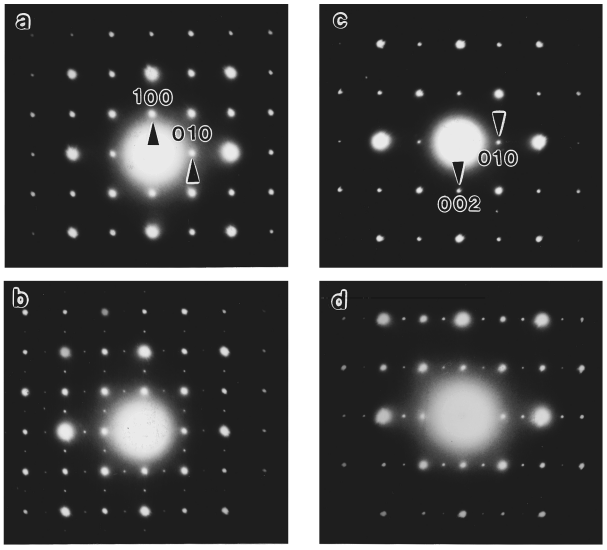

FIG. 3. Electron diffraction patterns of $Nd_{0.65}Ca_{0.35}MnO_3$ taken at 250 K (a),(c) and 170 K (b),(d) along [001] (a),(b) and [100] (c),(d) zone axes.

charge ordering occurs only in the *a-b* plane, but is frustrated along the *c* axis. The accompanying changes in lattice parameters across the charge ordering transition temperature T_{CO} have been observed by neutron diffraction, and the results will be published elsewhere.[13] Below T_{CO}, the electron diffraction patterns do not show any appreciable difference down to 120 K.

Upon cooling the sample with $x=0.35$, charge ordering occurs at $T_{CO}\approx 240$ K in zero field, while the material remains paramagnetic as confirmed by neutron scattering.[13] AF ordering takes place at $T_N\approx 160$ K, below which CMR of increasing magnitude occurs, as shown in Fig. 2(a). Furthermore, this particular AF ordering shows some remarkable characteristics. Ordinary AF ordering usually displays small magnetization that is linearly proportional to the applied field (H), and no hysteresis. As shown in Fig. 4, these characteristics are indeed observed in the present material in the initial magnetizing curve up to a threshold field (H_f). However, above H_f, the magnetization increases *suddenly* and without saturation up to 5 T. As the field is decreased from 5 T, M remains high until at a field much smaller than the initial H_f, it reduces to nearly zero for the AF state. At 5 K, as shown in Fig. 4(a), cycling H between ± 5 T, one obtains a *FM-like* loop. There is a strong irreversibility between the initial magnetization and the field-cycled magnetization. At higher temperatures, as shown in Fig. 4(b) at 30 K, the hysteresis loop consists of two substantial loops. The field-cycled magnetization more or less follows the initial magnetization. These unusual characteristics are reminiscent of the *metamagnetic* transition observed in some AF materials.

The phase diagram of the $x=0.35$ sample in the field-temperature plane is shown in Fig. 5. Upon cooling in zero field, the paramagnetic sample undergoes first a charge ordering (becomes CO-PM) near 240 K, followed by an AF ordering (becomes CO-AF) near 160 K. In a magnetic field up to 5 T, the charge ordering transition temperature T_{CO} (solid squares) and the Néel temperature T_N (open circles) are only slightly lowered. For the charge-ordered AF state, at

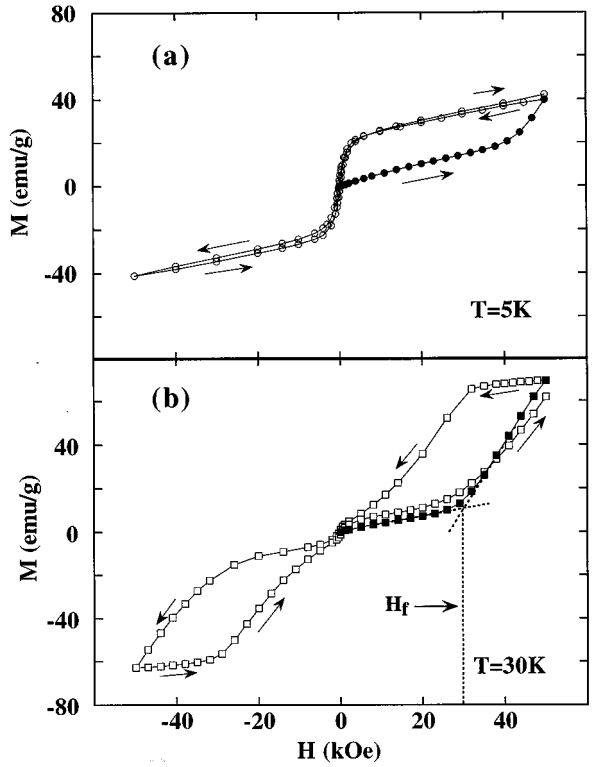

FIG. 4. Magnetic hysteresis loops of $Nd_{0.65}Ca_{0.35}MnO_3$ at (a) 5 K and (b) 30 K. Solid symbols indicate the initial magnetization. The threshold field H_f is determined from the interception of the linear portions of the initial magnetization, as shown in (b).

low temperatures, a field-induced AF-FM transition occurs at the threshold field H_f (solid circles). The value of H_f first decreases and then increases with increasing temperature. The threshold fields map out a region of FM ordering in the phase diagram. Note that only the values of the initial H_f are used for the phase boundary. As shown in Fig. 4, because of the metastable nature of the transition, once the system crosses from AF to FM, reducing the field back to below H_f does not return the system back to AF.

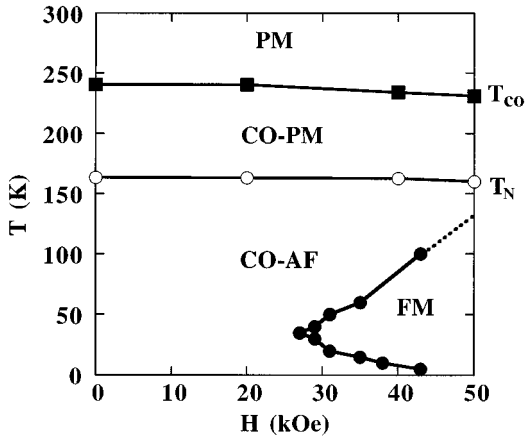

FIG. 5. Temperature-field phase diagram for $Nd_{0.65}Ca_{0.35}MnO_3$, showing the paramagnetic (PM), antiferromagnetic (AF), ferromagnetic (FM), and charge-ordered (CO) phases. The threshold field H_f (solid circles) is taken to be the boundary between AF and FM. Near 5 T H_f cannot be determined accurately; its values are shown only as the dashed line.

The interesting transport and unusual magnetic behaviors exhibited in the present system originate from the competition between mechanisms that promote electron itineracy and those that favor localization. Double exchange facilitates electron itineracy and ferromagnetism. In competition with DE, a few mechanisms favor electron localization. The Jahn-Teller distortion of the Mn^{3+} ($3d^4$) state lowers the energy of the e_g electron and impedes it from hopping to the undistorted e_g state of Mn^{4+}, leading to the formation of polarons. The mutual repulsion between charge carriers accommodates charge ordering at low temperatures. The AF superexchange gives rise to antiparallel core spin alignment which prevents hopping of spin-carrying e_g electrons. These effects lead to charge localization, ultimately charge ordering, and antiferromagnetism.

In systems like $La_{1-x}Ca_xMnO_3$ ($0.20 \leqslant x \leqslant 0.45$),[15] DE dominates the competition below T_C; metallic conduction and FM therefore prevail. Above T_C, electron localization takes place, resulting in semiconducting and PM behavior. In the present system, the replacement of La by the smaller Nd introduces a larger lattice distortion, reduces the Mn-O-Mn bond angle in particular, and thus weakens DE.[4] The competition now favors charge localization in the *whole* temperature range in zero field. Consequently, only semiconducting behavior can be observed in all compositions $0 \leqslant x \leqslant 1$. The resistivity values are larger than those in La- or Pr-based systems.[4,15] Furthermore, charge ordering transition has been observed in a broad composition range of $0.30 \leqslant x \leqslant 0.80$. Finally, AF, instead of FM, occurs at low temperatures in the same composition range.

Application of a magnetic field tends to align the core spins, thus enhancing DE. Focusing on the $x = 0.35$ sample (Fig. 5) again, in the PM state, the magnetic field only slightly aligns the random core spins, and the value of T_{CO} is marginally reduced. In the charge-ordered AF state, however, the effect of the field-enhanced DE becomes overwhelming. Consequently, the system is driven into a metastable FM state, giving rise to CMR. The metastable nature of this FM state is responsible for the strong field irreversibility observed at low temperatures ($T < 30$ K), as shown in Fig. 4.

Very recently, results of the related $Nd_{1/2}Sr_{1/2}MnO_3$ (Ref. 16) and $Pr_{1-x}Ca_xMnO_3$ ($x \leqslant 0.5$) (Ref. 17) systems have appeared. The results, especially those from the $Pr_{1-x}Ca_xMnO_3$ system obtained from single crystals, are similar to the present study using polycrystalline samples. Both Pr and Nd have similar ionic sizes which are smaller than that of La; their compounds thus have larger lattice distortions than the La-based one. Double exchange is effectively reduced in both cases, leading to the unusual transport and magnetic behaviors seen. The consistency between these separate studies on different systems well illustrates the relative significance of double exchange and the other mechanisms in determining the properties of the materials. It also suggests that the lattice effect can be used as a primary tool to tune the CMR. Furthermore, some earlier studies have shown drastically different properties between single-crystal and polycrystalline materials,[18,9] indicating significant effects of grain boundaries on CMR. The similarities in results between the present polycrystalline $Nd_{1-x}Ca_xMnO_3$ samples and the single crystals of $Pr_{1-x}Ca_xMnO_3$ and $Nd_{1/2}Sr_{1/2}MnO_3$, however suggest that grain boundaries do not necessarily affect CMR.

In summary, we have observed a two-dimensional charge ordering transition in $Nd_{1-x}Ca_xMnO_3$ over a large composition range $0.30 \leqslant x \leqslant 0.80$, accompanied by an abrupt increase in resistivity. For $0.33 \leqslant x \leqslant 0.40$, at low temperatures, the magnetic field induces a metastable first-order phase transition from an AF semiconductor to FM metal and reduces the resistance by several orders of magnitude. Our results show the close competition between double exchange and the mechanisms of electron-phonon, Coulomb interaction, and antiferromagnetic superexchange.

The authors thank Dr. C. Broholm for making the neutron scattering results available before publication. This work is supported by NSF Grant No. DMR 95-01195.

[1] See, e.g., R. M. Kusters *et al.*, Physica B **155**, 362 (1989); R. von Helmolt *et al.*, Phys. Rev. Lett. **71**, 2331 (1993); K. Chahara *et al.*, Appl. Phys. Lett. **63**, 1990 (1993); S. Jin *et al.*, Science **264**, 413 (1994).

[2] C. Zener, Phys. Rev. **82**, 403 (1951); P.-G. de Gennes, *ibid.* **118**, 141 (1960).

[3] J. B. Torrance, P. Lacorre, and A. I. Nazzal, Phys. Rev. B **45**, 8209 (1992).

[4] H. Y. Hwang *et al.*, Phys. Rev. Lett. **75**, 914 (1995).

[5] A. J. Millis, P. B. Littlewood, and B. I. Shraiman, Phys. Rev. Lett. **74**, 5144 (1995).

[6] A. J. Millis, B. I. Shraiman, and R. Mueller (unpublished).

[7] C. H. Chen, S-W. Cheong, and A. S. Cooper, Phys. Rev. Lett. **71**, 2461 (1993).

[8] Y. Moritomo *et al.*, Phys. Rev. B **51**, 3297 (1995).

[9] Y. Tomioka *et al.*, Phys. Rev. Lett. **74**, 5108 (1995).

[10] A. P. Ramirez *et al.*, Phys. Rev. Lett. **76**, 3188 (1996).

[11] A. Asamitsu *et al.*, Nature **373**, 407 (1995).

[12] M. R. Ibarra *et al.*, Phys. Rev. Lett. **75**, 3541 (1995).

[13] K. Liu *et al.* (unpublished).

[14] R. D. Shannon, Acta Crystallogr. A **32**, 751 (1976).

[15] P. Schiffer, A. P. Ramirez, W. Bao, and S-W. Cheong, Phys. Rev. Lett. **75**, 3336 (1995).

[16] H. Kuwahara *et al.*, Science **270**, 961 (1995).

[17] H. Yoshizawa *et al.*, Phys. Rev. B **52**, R13 145 (1995); Y. Tomioka *et al.*, *ibid.* **53**, R1689 (1996).

[18] M. McMormack *et al.*, Appl. Phys. Lett. **64**, 3045 (1994).